ISSN 0915-633X

INTERNATIONAL ATOMIC ENERGY AGENCY

18th IAEA Fusion Energy Conference
Sorrento, Italy, 4 to 10 October 2000

IAEA-CN-77/TH6/2

NATIONAL INSTITUTE FOR FUSION SCIENCE

Fokker-Planck Simulation Study of Alfvén Eigenmode Burst

Todo, Y., Watanabe, T.-H., Park, H.-B., Sato, T.

(Received - Aug. 30, 2000)

NIFS-645 Sep. 2000

RESEARCH REPORT
NIFS Series

TOKI, JAPAN

INTERNATIONAL ATOMIC ENERGY AGENCY

18th IAEA Fusion Energy Conference
Sorrento, Italy, 4 to 10 October 2000

IAEA-CN-77/TH6/2

Fokker-Planck Simulation Study of Alfvén Eigenmode Burst

Y. Todo, T.-H. Watanabe, Hyoung-Bin Park[†], and T. Sato

Theory and Computer Simulation Center,
National Institute for Fusion Science, 322-6 Oroshi-cho, Toki-shi 509-5292, Japan

e-mail contact of main author: todo@nifs.ac.jp

Abstract. Recurrent bursts of toroidicity-induced Alfvén eigenmodes (TAE) are reproduced with the Fokker-Planck-magnetohydrodynamic simulation where fast-ion source and slowing down are incorporated self-consistently. The bursts take place with a regular time interval and behaviors of all the TAEs are synchronized. The fast-ion transport due to TAE activity spatially broadens the classical fast-ion distribution and significantly reduces its peak value. Only a small change of the distribution takes place with each burst, leading to loss of a small fraction of fast ions. The system stays close to the marginal stability state established through the interplay of fast-ion source, slowing down, and TAE activity.

1. Introduction

Toroidicity-induced Alfvén eigenmode (TAE) is a shear-Alfvén eigenmode in toroidal plasmas [1]. TAEs can be destabilized by fast ions which have velocities comparable to Alfvén velocity. Several years ago, recurrent bursts of TAEs were observed with drops in neutron emission during neutral beam injection in TFTR [2] and DIII-D [3]. The drops in neutron emission have been recognized as a manifestation of TAE-induced fast-ion loss. Nonlinear evolution of TAEs, especially the TAE burst, is an important issue for fusion reactors, since successful confinement of energetic alpha particles is required for self-sustained operation. It must be noted that multiple TAEs are destabilized during TAE burst and bursts take place at regular time intervals. The fraction of the drop in neutron emission to the total emission in TFTR plasma was typically less than 10% (Fig. 4 of Ref. [2]).

It was demonstrated with numerical simulation of a system reduced by a mapping method that the resonance overlap of multiple TAEs enhances the energy release from fast ions to TAEs and synchronizes the behavior of multiple TAEs [4]. More realistic simulations which incorporate the TAE mode structure and the resonance conditions in a realistic tokamak are needed to make more quantitative comparisons with experiment. Recently, Candy *et al.* [5] carried out δf particle simulation where linear eigenmodes are coupled with fast-ion dynamics and reproduced a bursting behavior of TAE with realistic plasma parameters. In Ref. [5] a single dominant TAE which grows up to an amplitude of $\delta B/B \sim 2 \times 10^{-2}$ creates orbit islands in the phase space. Overlap of orbit islands makes the entire phase space stochastic and allows rapid conversion of particle free energy to wave energy. The large stochastic region causes a complete flattening of the fast-ion density profile. Although this is one possible mechanism of periodic bursts due to neutral beam injection, it seems unlikely for TFTR and DIII-D experiments since multiple modes were observed.

Another simulation method, namely the Fokker-Planck-magnetohydrodynamic (MHD) simulation, has been developed [6, 7, 8]. Results of the Fokker-Planck-MHD simulation

[†]Present address: Samsung Advanced Institute of Technology, P.O. Box 111, Suwon 440-600, Korea

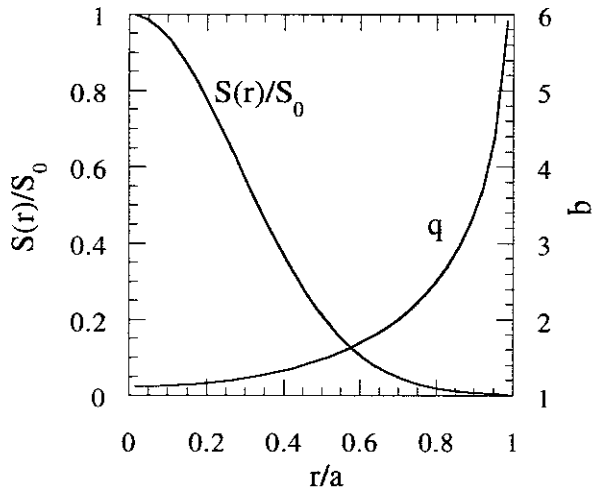

FIG. 1. The fast-ion source profile and the q-profile as functions of the minor radius.

have shown that TAE bursts take place if the fast-ion slowing-down time is sufficiently longer than the TAE damping time and the heating power is sufficiently high. In this paper we report new simulation results where a few percent of fast ions are lost with each TAE bursts and all the TAEs have a synchronized behavior. We analyze the time evolution of fast-ion distribution and show that the change of distribution with each burst is relatively small compared with the distribution itself.

2. Simulation Model

A kinetic-MHD hybrid simulation model, which was used to investigate the saturation mechanism of collisionless fast-ion driven TAE [9, 10], is employed. In this model plasma is divided into two parts, the background plasma and fast ions. The background plasma is described by the nonlinear full MHD equations and the electromagnetic field is given by the MHD description. This approximation is reasonable under the condition that the fast-ion density is much less than the background plasma density. The MHD equations are,

$$\frac{\partial \rho}{\partial t} = -\nabla \cdot (\rho \mathbf{v}), \tag{1}$$

$$\rho \frac{\partial}{\partial t}\mathbf{v} + \rho \mathbf{v} \cdot \nabla \mathbf{v} = -\nabla p + \tfrac{1}{\mu_0}(\nabla \times \mathbf{B}) \times \mathbf{B} + \nu \rho \triangle \mathbf{v}, \tag{2}$$

$$\frac{\partial \mathbf{B}}{\partial t} = -\nabla \times \mathbf{E}, \tag{3}$$

$$\frac{\partial p}{\partial t} = -\nabla \cdot (p\mathbf{v}) - (\gamma - 1) p \nabla \cdot \mathbf{v}, \tag{4}$$

$$\mathbf{E} = -\mathbf{v} \times \mathbf{B}, \tag{5}$$

where μ_0 is the vacuum magnetic permeability and γ is the adiabatic constant, and all other quantities are conventional.

We use a four-dimensional phase space (R, φ, z, v), where v is the parallel velocity and (R, φ, z) are the cylindrical coordinates. Only the parallel velocity component is taken

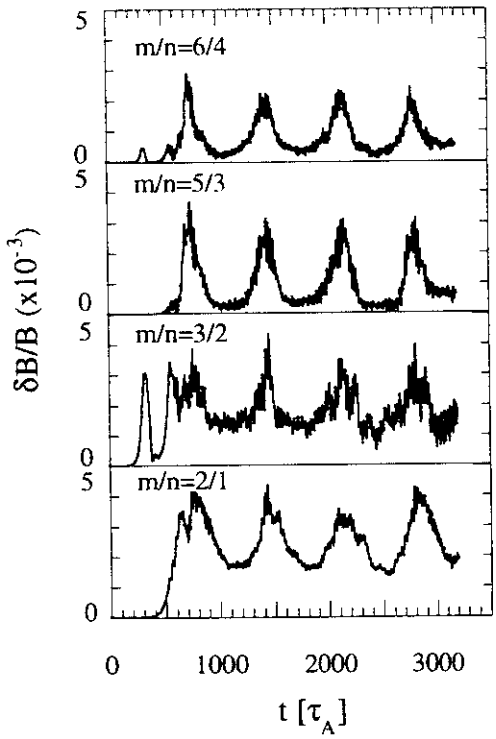

FIG. 2. Time evolutions of radial magnetic field fluctuations of $m/n = 2/1, 3/2, 5/3$, and $6/4$ harmonics.

into account for simplicity. We, however, adopt a Jacobian for the three-dimensional velocity space to be consistent with the slowing-down term. The grid numbers used are $(65, 72, 65, 20)$ for (R, φ, z, v) coordinates, respectively. The initial condition is an MHD equilibrium where the aspect ratio is 3. For analysis of simulation data a flux coordinate system (r, φ, θ) is constructed. The unit of length is the Larmor radius of a fast ion whose velocity is equal to the Alfvén velocity ($\equiv v_A m_f/q_f B$) at the initial magnetic axis. The minor radius denoted as a is taken to be 16, and the simulation domain is ($32 \leq R \leq 64$, $0 \leq z \leq 32$). The initial magnetic axis locates at ($R = R_0 \equiv 50.5, z = z_0 \equiv 16$). The unit of time is the Alfvén time ($\tau_A \equiv R_0/v_A$).

The effect of fast ions on the MHD fluid is taken into account in the MHD momentum equation through the fast-ion perpendicular current [10, 11]. Time evolution of the fast-ion distribution is described by the following Fokker-Planck equation:

$$\begin{aligned}
\frac{\partial}{\partial t} f &= -\nabla \cdot (\mathbf{v}_D) - \frac{\partial}{v^2 \partial v} v^2 a_H f \\
&+ \frac{1}{\tau_s} \frac{\partial}{v^2 \partial v} (v_{\rm crit}^3 + v^3) f + \frac{S(\mathbf{x})}{v^2} \delta(v - v_0), \qquad (6) \\
\mathbf{v}_D &= \frac{v}{B} \left[\mathbf{B} + \frac{m_f}{q_f} v \nabla \times \mathbf{b} \right] + \frac{1}{B} [\mathbf{E} \times \mathbf{b}], \qquad (7) \\
\mathbf{b} &= \mathbf{B}/B, \qquad (8) \\
a_H &= \frac{v}{B} \nabla \times \mathbf{b} \cdot \mathbf{E}, \qquad (9) \\
S(\mathbf{x}) &= S_0 \exp\{-\alpha^2 [(R - R_0)^2 + (z - z_0)^2]\} \, . \qquad (10)
\end{aligned}$$

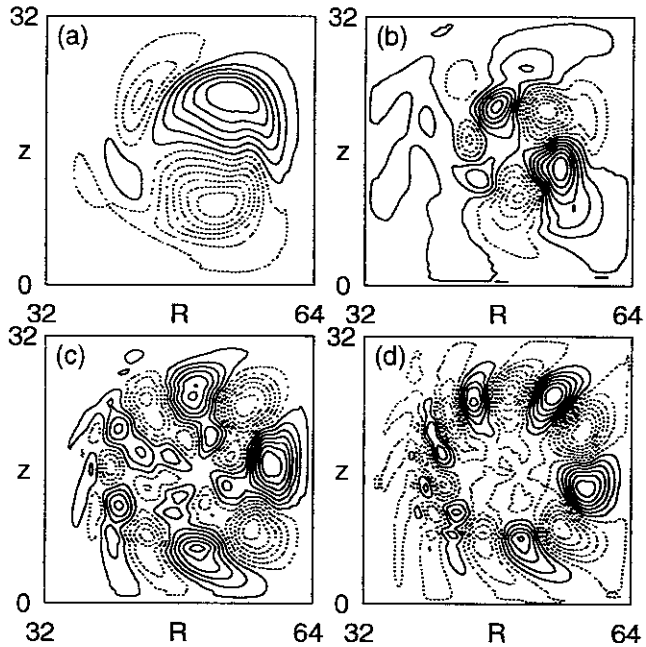

FIG. 3. Contours of the toroidal electric field on a poloidal cross section at $t = 713\tau_A$ for toroidal mode numbers of (a) $n = 1$, (b) $n = 2$, (c) $n = 3$, and (d) $n = 4$.

Here, $v_{\rm crit}$ is the critical velocity above which the collision with background electrons dominates over that with background ions, and v_0 is the birth velocity of fast ions. We choose $v_{\rm crit} = 0.3v_A$ and $v_0 = 1.5v_A$, respectively. On the right-hand-side of Eq. (6), the slowing-down time is denoted as τ_s and chosen $\tau_s = 2000\tau_A$. The fourth term of Eq. (6) represents the source of fast ions. In Eq. (10) α is set to be equal to $1/0.4a$, and S_0 is chosen so that the central fast-ion beta value of the classical distribution is 2%. The classical distribution is realized through a balance between the source and the slowing down and is a steady solution without any nonaxisymmetric modes, especially TAE activities. The source profile is shown in Fig. 1 with the q-profile. A finite viscosity of $2 \times 10^{-5} v_A R_0$ is considered to mimic the damping of TAEs. It yields, for example, an e-folding damping time of $130\tau_A$ for an $n = 2$ TAE which is the most unstable TAE in the simulation described below. The Fokker-Planck equation and the full MHD equations are solved with a finite difference method of a fourth-order accuracy in space and time.

3. Results

Time evolutions of radial magnetic fluctuation harmonics in the simulation results are shown in Fig. 2. Four TAEs with the toroidal mode numbers from 1 to 4 are destabilized. Figure 3 shows contours of the toroidal electric field of the four TAEs on a poloidal cross section at $t = 713$. The frequencies of $m/n = 2/1, 3/2, 5/3$, and $6/4$ harmonics are $0.28\omega_A$, $0.35\omega_A$, $0.28\omega_A$, and $0.30\omega_A$, respectively, and these are reasonable values for TAE. At $t = 0$ there is no fast ion and as time passes fast ions gradually accumulate due to the fast-ion source. Accumulated fast ions destabilize the $n = 2$ TAE first at $t = 300$. Later than

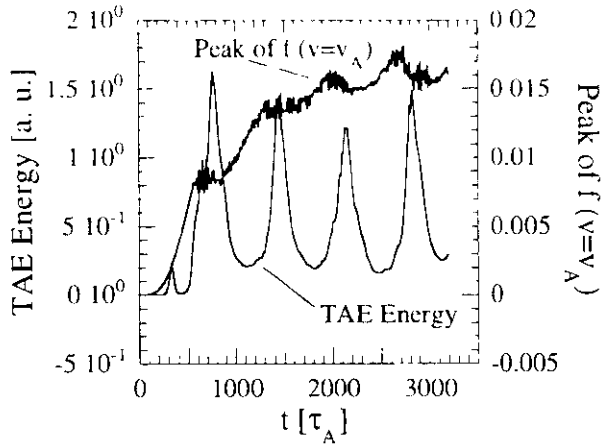

FIG. 4. Time evolutions of total TAE energy and the fast-ion distribution peak value for $v = v_A$.

this precursory growth of the $n = 2$ TAE. the other TAEs grow up to levels comparable to that of the $n = 2$ TAE and behaviors of all the TAEs are synchronized.

We turn to the detailed behavior of the burst. In Fig. 4 we show time evolutions of the total TAE energy and the peak value of the fast-ion distribution function at $v = v_A$. We can see correlation between drop in fast-ion distribution and growth of TAE energy. Figure 5 shows as a bird's-eye view plot in (t, R) space the time evolution of fast-ion distribution averaged in the toroidal angle with $v = v_A$ on the midplane. Bright parts are regions flattened due to TAE activity. TAEs flatten the fast-ion spatial distribution through the $\mathbf{E} \times \mathbf{B}$ trapping. In contrast to the bright flattened regions, we can see dark regions elongated in R-direction around $t = 700, 1400, 2100$, and 2800 accompanying the TAE bursts. These dark regions are rapid temporal changes of the fast-ion distribution. To see more clearly, the fast-ion distributions are plotted in Fig. 6 as functions of the major radius (a) at $t = 2000$ (before burst) and (b) at $t = 2300$ (after burst) with the classical distribution which is a steady solution obtained with a simulation suppressing any nonaxisymmetric modes, especially TAE activities. Comparing the distributions before and after the burst, it can be seen that the fast ions are transported outwards across a distribution precipice at $R = 59$. We must pay attention to the following: (1) compared with the classical distribution, the two distributions before and after the burst are significantly broadened in the radial direction and their peak values are also reduced by half, (2) the change of the distribution function during the burst is relatively small compared with the distribution itself. The former means that the fast-ion distribution is significantly affected by the TAE activity. The latter indicates that the difference between the unstable state (before burst) and the stable state (after burst) is small. Thus, we conclude that the system stays close to the marginal stability state which is established through the interplay of fast-ion source, slowing down, and multiple TAEs' activity. This is a behavior different from that found in the particle simulation [5] where with each burst the fast ion density is completely flattened from a steep-gradient state.

We show the time evolutions of total fast-ion energy and total TAE energy in Fig. 7. It can be seen that the drops in fast-ion energy of 3% take place accompanying TAE bursts.

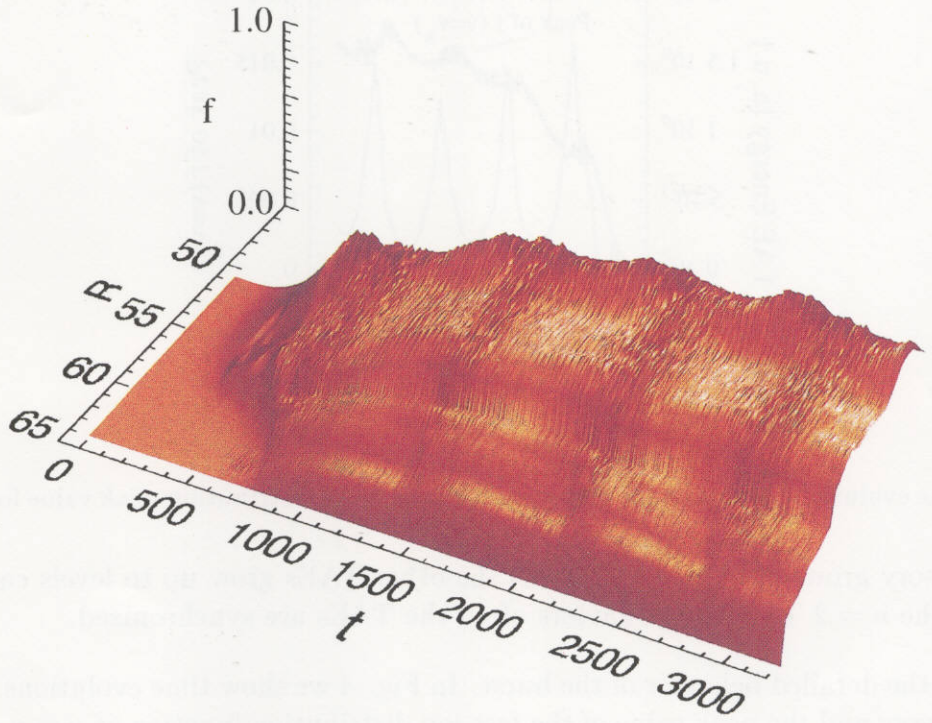

FIG. 5. Bird's-eye view plot of the time evolution of the fast-ion distribution on (t, R) plane. The distribution is averaged in toroidal angle on the midplane ($z = 16$) at $v = v_A$.

These drops are due to fast-ion loss and are similar to those in neutron emission in neutral-beam-injected plasmas [2, 3]. The fast-ion loss is a result of the outward transport of fast ions.

4. Discussion and Summary

TAE burst with such a loss of small fraction of fast ions has been discussed in the resonance overlap scenario of multiple modes [12]. The synchronization of multiple TAEs in the present simulation results is consistent with the resonance overlap scenario [4]. Bursting behavior of TAEs has been explained by the simple predator-prey model [13]. It, however, cannot discuss many characteristics revealed in the present simulation such as the synchronization of multiple TAEs and the spatial broadening of the fast-ion distribution. Furthermore, we would like to emphasize that the present simulation is based on the fundamental physics principles.

Finally, let us compare the simulation and experimental results. If we apply the parameters $B_0 = 1$ [T], $R_0 = 2.4$ [m], and $n_0 = 3 \times 10^{19}$ [m^{-3}], which are typical for the TAE bursts in the TFTR deuterium plasma [2], the bursting period of 700 τ_A in the simulation results corresponds to 0.6 [ms]. This is shorter than the typical experimental value of 2 [ms]. This discrepancy arises from the shorter heating time scale, which we define as the ratio of the accumulated fast-ion energy to the heating power, in the present simulation than in the typical TFTR experiment by a factor of 7. The simulation time step is limited by the time for the MHD fast mode to propagate the grid size, whereas we must simulate

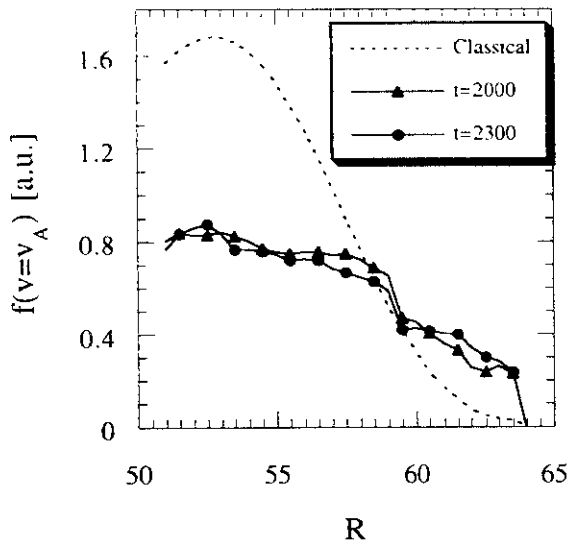

FIG. 6. Fast-ion distributions before (t = 2000) and after (t = 2300) the TAE burst and the classical distribution, as functions of the major radius.

a time span of the several burst periods which is roughly comparable to the heating time scale. The purpose that we have employed such a short heating time scale is to reduce the time span simulated and make the CPU time reasonable. Nevertheless, even on the present simulation run we have spent 70 hours using 15 CPU of NEC SX-4/64M2. The short burst period in simulation results also leads to the small ratio of the maximum amplitude to the minimum amplitude of $n = 1$ and 2 TAEs, since these modes do not have enough time to damp in the short quiescent period. Therefore, more realistic simulation is needed to make more strict comparison. We must note, however, that the volume-averaged fast-ion beta value at the end of the simulation is 0.6% which is comparable to the experiment. Since the fast-ion beta value is crucial for the TAE evolution, we have chosen the slowing-down time and the source intensity S_0 to meet the fast-ion beta with experiment.

In conclusion, we have successfully reproduced the recurrent TAE burst and TAE-induced fast-ion loss with the Fokker-Planck-MHD simulation. The TAE bursts take place at a regular time interval and behaviors of all the TAEs are synchronized. The fast-ion transport due to TAE activity spatially broadens the classical fast-ion distribution and significantly reduces its peak value. Only a small change of the distribution takes place with each burst, leading to loss of a small fraction of fast ions. The synchronization of multiple TAEs and the loss of small fraction of fast ions are consistent with the resonance overlap scenario. The system stays close to the marginal stability state established through the interplay of fast-ion source. slowing down, and TAE activity.

ACKNOWLEDGMENTS

Numerical computations were performed at the Man-Machine Interactive System for Simulation (MISSION) of National Institute for Fusion Science. This work was partially sup-

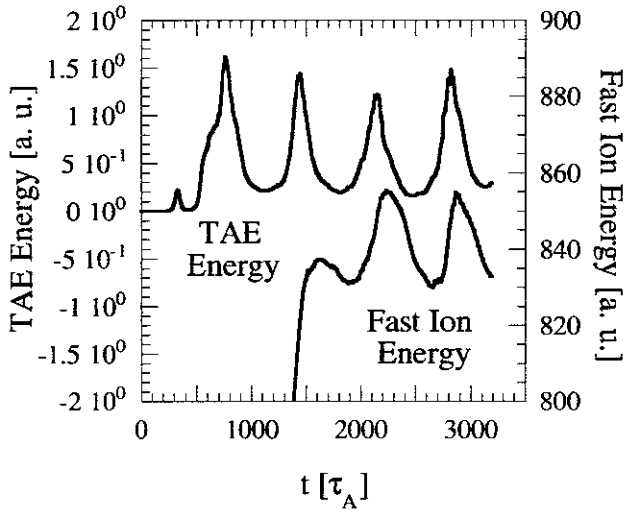

FIG. 7. Time evolutions of total TAE energy and fast-ion energy.

ported by Grant-in-Aid of the Ministry of Education, Science, Sports, and Culture (No. 11780363).

References

[1] C. Z. Cheng and M. S. Chance, Phys.Fluids **29**, 3659 (1986).

[2] K. L. Wong *et al.*, Phys. Rev. Lett. **66**, 1874 (1991).

[3] H. H. Duong *et al.*, Nucl. Fusion **33**, 749 (1993).

[4] H. L. Berk, B. N. Breizman, and M. S. Pekker, Nucl. Fusion **35**, 1713 (1995).

[5] J. Candy *et al.*, Phys. Plasmas **6**, 1822 (1999).

[6] Y. Todo and T. Sato, in *Theory of Fusion Plasmas, 1998*, Varenna (Società Italiana di Fisica, Bologna, 1999), p. 229.

[7] Y. Todo and T. Sato, in *Fusion Energy, 1998*, Yokohama (International Atomic Energy Agency, Vienna, 1999), Vol. 4, p. 1577.

[8] Y. Todo and T. Sato, J. Plasma Fusion Res. SERIES **2**, 263 (1999).

[9] G. Y. Fu and W. Park, Phys. Rev. Lett. **74**, 1594 (1995).

[10] Y. Todo *et al.*, Phys. Plasmas **2**, 2711 (1995).

[11] Y. Todo and T. Sato, Phys. Plasmas **5**, 1321 (1998)

[12] H. L. Berk and B. N. Breizman, in *Theory of Fusion Plasmas, 1998*, Varenna (Società Italiana di Fisica, Bologna, 1999), p. 283.

[13] W. W. Heidbrink *et al.*, Phys. Fluids B **5**, 2176 (1993).

Recent Issues of NIFS Series

NIFS-581 M. Tanaka, A. Yu Grosberg and T. Tanaka,
Comparison of Multichain Coulomb Polymers in Isolated and Periodic Systems: Molecular Dynamics Study; Jan. 1999

NIFS-582 VS Chan and S. Murakami,
Self-Consistent Electric Field Effect on Electron Transport of ECH Plasmas, Feb 1999

NIFS-583 M. Yokoyama, N. Nakajima, M. Okamoto, Y. Nakamura and M. Wakatani,
Roles of Bumpy Field on Collisionless Particle Confinement in Helical-Axis Heliotrons, Feb. 1999

NIFS-584 T.-H. Watanabe, T. Hayashi, T. Sato, M. Yamada and H. Ji,
Modeling of Magnetic Island Formation in Magnetic Reconnection Experiment; Feb 1999

NIFS-585 R. Kumazawa, T. Mutoh, T. Seki, F. Shinpo, G. Nomura, T. Ido, T. Watari, Jean-Marie Noterdaeme and Yangping Zhao,
Liquid Stub Tuner for Ion Cyclotron Heating, Mar. 1999

NIFS-586 A. Sagara, M. Iima, S. Inagaki, N. Inoue, H. Suzuki, K. Tsuzuki, S. Masuzaki, J. Miyazawa, S. Morita, Y. Nakamura, N. Noda, B. Peterson, S. Sakakibara, T. Shimozuma, H. Yamada, K. Akaishi, H. Chikaraishi, H. Funaba, O. Kaneko, K. Kawahata, A. Komori, N. Ohyabu, O. Motojima, LHD Exp. Group 1, LHD Exp. Group 2,
Wall Conditioning at the Starting Phase of LHD, Mar. 1999

NIFS-587 T. Nakamura and T. Yabe,
Cubic Interpolated Propagation Scheme for Solving the Hyper-Dimensional Vlasov-Poisson Equation in Phase Space; Mar. 1999

NIFS-588 W.X. Wnag, N. Nakajima, S. Murakami and M. Okamoto,
An Accurate δf Method for Neoclassical Transport Calculation; Mar. 1999

NIFS-589 K. Kishida, K. Araki, S. Kishiba and K. Suzuki,
Local or Nonlocal? Orthonormal Divergence-free Wavelet Analysis of Nonlinear Interactions in Turbulence; Mar 1999

NIFS-590 K. Araki, K. Suzuki, K. Kishida and S. Kishiba,
Multiresolution Approximation of the Vector Fields on T^3; Mar. 1999

NIFS-591 K. Yamazaki, H. Yamada, K.Y. Watanabe, K. Nishimura, S. Yamaguchi, H. Nakanishi, A. Komori, H. Suzuki, T. Mito, H. Chikaraishi, K. Murai, O. Motojima and the LHD Group,
Overview of the Large Helical Device (LHD) Control System and Its First Operation; Apr. 1999

NIFS-592 T. Takahashi and Y. Nakao,
Thermonuclear Reactivity of D-T Fusion Plasma with Spin-Polarized Fuel; Apr 1999

NIFS-593 H. Sugama,
Damping of Toroidal Ion Temperature Gradient Modes; Apr 1999

NIFS-594 Xiaodong Li,
Analysis of Crowbar Action of High Voltage DC Power Supply in the LHD ICRF System, Apr 1999

NIFS-595 K. Nishimura, R. Horiuchi and T. Sato,
Drift-kink Instability Induced by Beam Ions in Field-reversed Configurations; Apr. 1999

NIFS-596 Y. Suzuki, T-H. Watanabe, T. Sato and T. Hayashi,
Three-dimensional Simulation Study of Compact Toroid Plasmoid Injection into Magnetized Plasmas; Apr 1999

NIFS-597 H. Sanuki, K. Itoh, M. Yokoyama, A. Fujisawa, K. Ida, S. Toda, S.-I. Itoh, M. Yagi and A. Fukuyama,
Possibility of Internal Transport Barrier Formation and Electric Field Bifurcation in LHD Plasma;
May 1999

NIFS-598 S. Nakazawa, N. Nakajima, M. Okamoto and N. Ohyabu,
One Dimensional Simulation on Stability of Detached Plasma in a Tokamak Divertor; June 1999

NIFS-599 S. Murakami, N. Nakajima, M. Okamoto and J. Nhrenberg,
Effect of Energetic Ion Loss on ICRF Heating Efficiency and Energy Confinement Time in Heliotrons;
June 1999

NIFS-600 R. Horiuchi and T. Sato,
Three-Dimensional Particle Simulation of Plasma Instabilities and Collisionless Reconnection in a Current Sheet;; June 1999

NIFS-601 W. Wang, M. Okamoto, N. Nakajima and S. Murakami,
Collisional Transport in a Plasma with Steep Gradients; June 1999

NIFS-602 T. Mutoh, R. Kumazawa, T. Saki, K. Saito, F. Simpo, G. Nomura, T. Watari, X. Jikang, G. Cattanei, H. Okada, K. Ohkubo, M. Sato, S. Kubo, T. Shimozuma, H. Idei, Y. Yoshimura, O. Kaneko, Y. Takeiri, M. Osakabe, Y. Oka, K. Tsumori, A. Komori, H. Yamada, K. Watanabe, S. Sakakibara, M. Shoji, R. Sakamoto, S. Inagaki, J. Miyazawa, S. Morita, K. Tanaka, B.J. Peterson, S. Murakami, T. Minami, S. Ohdachi, S. Kado, K. Narihara, H. Sasao, H. Suzuki, K. Kawahata, N. Ohyabu, Y. Nakamura, H. Funaba, S. Masuzaki, S. Muto, K. Sato, T. Morisaki, S. Sudo, Y. Nagayama, T. Watanabe, M. Sasao, K. Ida, N. Noda, K. Yamazaki, K. Akaishi, A. Sagara, K. Nishimura, T. Ozaki, K. Toi, O. Motojima, M. Fujiwara, A. Iiyoshi and LHD Exp. Group 1 and 2,
First ICRF Heating Experiment in the Large Helical Device; July 1999

NIFS-603 P.C. de Vries, Y. Nagayama, K. Kawahata, S. Inagaki, H. Sasao and K. Nagasaki,
Polarization of Electron Cyclotron Emission Spectra in LHD; July 1999

NIFS-604 W. Wang, N. Nakajima, M. Okamoto and S. Murakami,
δf Simulation of Ion Neoclassical Transport; July 1999

NIFS-605 T. Hayashi, N. Mizuguchi, T. Sato and the Complexity Simulation Group,
Numerical Simulation of Internal Reconnection Event in Spherical Tokamak; July 1999

NIFS-606 M. Okamoto, N. Nakajima and W. Wang,
On the Two Weighting Scheme for δf Collisional Transport Simulation; Aug. 1999

NIFS-607 O. Motojima, A.A. Shishkin, S. Inagaki, K.Y. Watanabe,
Possible Control Scenario of Radial Electric Field by Loss-Cone-Particle Injection into Helical Device; Aug. 1999

NIFS-608 R. Tanaka, T. Nakamura and T. Yabe,
Constructing Exactly Conservative Scheme in Non-conservative Form; Aug. 1999

NIFS-609 H. Sugama,
Gyrokinetic Field Theory; Aug. 1999

NIFS-610 M. Takechi, G. Matsunaga, S. Takagi, K.Ohkuni, K. Toi, M. Osakabe, M. Isobe, S. Okamura, K. Matsuoka, A. Fujisawa, H. Iguchi, S. Lee, T. Minami, K. Tanaka, Y. Yoshimura and CHS Group,
Core Localized Toroidal Alfven Eigenmodes Destabilized By Energetic Ions in the CHS Heliotron/Torsatron; Sep. 1999

NIFS-611 K. Ichiguchi,
MHD Equilibrium and Stability in Heliotron Plasmas; Sep. 1999

NIFS-612 Y. Sato, M. Yokoyama, M. Wakatani and V. D. Pusovitov,
Complete Suppression of Pfirsch-Schluter Current in a Toroidal l=3 Stellarator; Oct. 1999

NIFS-613 S. Wang, H Sanuki and H. Sugama,
Reduced Drift Kinetic Equation for Neoclassical Transport of Helical Plasmas in Ultra-low Collisionality Regime,Oct. 1999

NIFS-614 J Miyazawa, H Yamada, K. Yasui, S. Kato, N., Fukumoto, M Nagata and T Uyama,
Design of Spheromak Injector Using Conical Accelerator for Large Helical Device;Nov 1999

NIFS-615 M. Uchida, A. Fukuyama, K. Itoh, S-I Itoh and M. Yagi,
Analysis of Current Diffusive Ballooning Mode in Tokamaks; Dec 1999

NIFS-616 M. Tanaka, A.Yu Grosberg and T Tanaka,
Condensation and Swelling Behavior of Randomly Charged Multichain Polymers by Molecular Dynamics Simulations; Dec 1999

NIFS-617 S. Goto and S. Kida,
Sparseness of Nonlinear Coupling; Dec 1999

NIFS-618 M.M. Skoric, T. Sato, A. Maluckov and M.S. Jovanovic,
Complexity in Laser Plasma Instabilities Dec. 1999

NIFS-619 T.-H. Watanabe, H. Sugama and T Sato,
Non-dissipative Kinetic Simulation and Analytical Solution of Three-mode Equations of Ion Temperature Gradient Instability; Dec 1999

NIFS-620 Y. Oka, Y. Takeiri, Yu.I.Belchenko, M. Hamabe, O. Kaneko, K. Tsumori, M. Osakabe, E Asano, T. Kawamoto, R. Akiyama,
Optimization of Cs Deposition in the 1/3 Scale Hydrogen Negative Ion Source for LHD-NBI System ;Dec 1999

NIFS-621 Yu I. Belchenko, Y. Oka, O. Kaneko, Y Takeiri, A. Krivenko, M Osakabe, K Tsumori, E. Asano, T. Kawamoto, R. Akiyama,
Recovery of Cesium in the Hydrogen Negative Ion Sources; Dec. 1999

NIFS-622 Y. Oka, O. Kaneko, K. Tsumori, Y. Takeiri, M. Osakabe, T. Kawamoto, E. Asano, and R. Akiyama,
H- Ion Source Using a Localized Virtual Magnetic Filter in the Plasma Electrode: Type I LV Magnetic Filter: Dec. 1999

NIFS-623 M. Tanaka, S Kida, S. Yanase and G. Kawahara,
Zero-absolute-vorticity State in a Rotating Turbulent Shear Flow;Jan 2000

NIFS-624 F. Leuterer, S Kubo,
Electron Cyclotron Current Drive at $\omega \approx \omega_c$ with X-mode Launched from the Low Field Side; Feb. 2000

NIFS-625 K Nishimura,
Wakefield of a Charged Particulate Influenced by Emission Process of Secondary Electrons; Mar. 2000

NIFS-626 K Itoh, M Yagi, S.-I. Itoh, A Fukuyama,
On Turbulent Transport in Burning Plasmas; Mar. 2000

NIFS-627 K Itoh, S.-I. Itoh, L Giannone,
Modelling of Density Limit Phenomena in Toroidal Helical Plasmas; Mar. 2000

NIFS-628 K Akaishi, M. Nakasuga and Y. Funato,
True and Measured Outgassing Rates of a Vacuum Chamber with a Reversibly Absorbed Phase; Mar 2000

NIFS-629 T Yamagishi,

Effect of Weak Dissipation on a Drift Orbit Mapping; Mar 2000

NIFS-630 S. Toda, S.-I, Itoh, M. Yagi, A Fukuyama and K Itoh,
Spatial Structure of Compound Dither in L/H Transition; Mar. 2000

NIFS-631 N. Ishihara and S. Kida,
Axial and Equatorial Magnetic Dipoles Generated in a Rotating Spherical Shell; Mar 2000

NIFS-632 T. Kuroda, H. Sugama, R. Kanno and M. Okamoto,
Ion Temperature Gradient Modes in Toroidal Helical Systems; Apr. 2000

NIFS-633 V.D. Pustovitov,
Magnetic Diagnostics: General Principles and the Problem of Reconstruction of Plasma Current and Pressure Profiles in Toroidal Systems; Apr. 2000

NIFS-634 A.B. Mikhailovskii, S.V. Konovalov, V.D. Pustovitov and V.S. Tsypin,
Mechanism of Viscosity Effect on Magnetic Island Rotation; Apr. 2000

NIFS-635 H. Naitou, T. Kuramoto, T. Kobayashi, M. Yagi, S. Tokuda and T. Matsumoto,
Stabilization of Kinetic Internal Kink Mode by Ion Diamagnetic Effects; Apr. 2000

NIFS-636 A. Kageyama and S. Kida,
A Spectral Method in Spherical Coordinates with Coordinate Singularity at the Origin; Apr. 2000

NIFS-637 R. Horiuchi, W. Pei and T. Sato,
Collisionless Driven Reconnection in an Open System, June 2000

NIFS-638 K. Nagaoka, A. Okamoto, S. Yoshimura and M.Y. Tanaka,
Plasma Flow Measurement Using Directional Langmuir Probe under Weakly Ion-Magnetized Conditions; July 2000

NIFS-639 Alexei Ivanov,
Scaling of the Distribution Function and the Critical Exponents near the Point of a Marginal Stability under the Vlasov-Poisson Equations; Aug. 2000

NIFS-640 K. Ohi, H. Naitou, Y. Tauchi, O. Fukumasa,
Observation of the Limit Cycle in the Asymmetric Plasma Divided by the Magnetic Filter; Aug. 2000

NIFS-641 H. Momota, G.H. Miley and J. Nadler,
Direct Energy Conversion for IEC Propulsions; Aug. 2000

NIFS-642 Y. Kondoh, T Takahashi and H. Momota,
Revisit to the Helicity and the Generalized Self-organization Theory; Sep. 2000

NIFS-643 H. Soltwisch, K. Tanaka,
Changes of the Electron Density Distribution during MHD Activity in CHS Sep. 2000

NIFS-644 Fujisawa, A., Iguchi, H., Minami, T., Yoshimura, Y., Sanuki, H., Itoh, K., Isobe, M., Nishimura, S., Tanaka, K., Osakabe, M., Nomura, I., Ida, K., Okamura, S., Toi, K., Kado, S., Akiyama, R., Shimizu, A., Takahashi, C., Kojima, M., Matsuoka, K., Hamada, Y., Fujiwara, M.,
Observation of Bifucation Property of Radial Electric Field Using a Heavy Ion Beam Probe; Sep. 2000
(IAEA-CN-77/ EX6/6)

NIFS-645 Todo, Y., Watanabe, T.-H., Park, H.-B., Sato, T.,
Fokker-Planck Simulation Study of Alfvén Eigenmode Burst; Sep. 2000
(IAEA-CN-77/ TH6/2)